The Reduced Pressure Test as a Measuring Tool in the Evaluation of Porosity/Hydrogen Content in Al-7 Wt pct Si-10 Vol pct SiC(p) Metal Matrix Composite

A.M. SAMUEL and F.H. SAMUEL

Porosity is one of the important factors critical to the production of optimum aluminum alloy castings. Hydrogen is mainly responsible for the "gas porosity" in such castings, which is also affected by other factors including melt cleanliness. The importance, therefore, of obtaining a reliable estimate of the melt hydrogen level prior to casting has led to the development of several techniques, among which the reduced pressure test (RPT), basically a comparative, qualitative test, appears to be the one popularly used in foundries due to its simplicity and easy adaptation to the foundry floor. Attempts have been made to quantify the test by correlating the densities of reduced pressure samples with the hydrogen contents of their melts. In the present study, the RPT was tested as a means of determining the hydrogen content in Al-7 wt pct Si-10 vol pct SiC composite melts as part of an on-going study being carried out in our laboratories on such composites. The results reveal that rather than indicating the hydrogen content of the melt, the RPT is a better indicator of the porosity content of the cast sample and can be employed as a melt quality measuring tool, provided the sample density is correctly related to said porosity. Qualitative analysis is substantiated throughout by pore size and distribution data obtained from image analysis. It is also found that compared to the unreinforced A356 matrix alloy, the composite material has a beneficial effect on the formation of porosity due to the tendency of the SiC reinforcement particles to restrict the growth of the pores. This, coupled with the microporosity associated with the presence of the SiC particles, results in the skewed pore size distribution curves typically observed for the composite samples.

I. INTRODUCTION

IN the production of optimum aluminum alloy castings, porosity is one of the major factors critical to the quality. The presence of porosity, inevitable to a certain extent in any casting, can be very detrimental in terms of surface quality and a deterioration in the mechanical properties and corrosion resistance. Hydrogen, the only gas capable of dissolving to a significant extent in molten aluminum but exhibiting very low solubility in the solid state, is basically responsible for the "gas porosity" in a casting as opposed to the "shrinkage porosity" that results from the volume shrinkage associated with solidification.[1] Other factors can also influence gas porosity formation, like the pressure during solidification, the chemical composition and solidification range of the alloy, and the solidification or cooling rate. Melt cleanliness, with particular regard to the presence of oxides and inclusions, is also being recognized as an important factor in that it influences hydrogen gas nucleation.[2,3,4] It becomes important, therefore, to control the hydrogen level of the melt in order to control the quality of the resultant casting.

The need to obtain a reliably accurate estimate of the hydrogen level in the melt prior to casting has led to the development of many techniques.[5] Among these, the reduced pressure test (RPT), also known as the Straube-Pfeiffer or the vacuum gas test, appears to be the one most widely used in foundries.[6] Essentially, the test consists of solidifying a sample of the melt under reduced pressure (usually in the 50 to 100 mm Hg range). This encourages pore formation, the pores expanding due to the lowered pressure and providing a much more porous sample than under atmospheric conditions of solidification. The product, a cup-shaped specimen, permits the gas level to be assessed in three ways: (a) viewing the top of the sample and judging a puffed up surface as corresponding to a heavy gas content in comparison to a smooth or concave surface representing a low level; (b) sectioning the sample, examining the roughly polished surface for porosity and comparing with a photographic standard; and (c) finer polishing of the sectioned half in order to better observe the porosity profile through the use of sophisticated means such as image analysis. A schematic representation of the procedure is shown in Figure 1.

Although popularly used in aluminum foundries over the years, the RPT is basically a comparative, qualitative test. Attempts have been made to quantify the test, mainly by Rosenthal, Lipson and co-workers[7,8] in the 1960s and, more recently (1989 to 1991), by Gruzleski and co-workers.[9,10] The quantification has been attempted through correlating the densities of reduced pressure samples with the hydrogen contents of their respective melts (monitored by the Telegas method) in order to obtain a reliable quantitative estimate of the gas level from the RPT results. However, success is limited to the alloy in question and its solidification range and freezing mechanism, as demonstrated by La Orchan *et al.* for A356 and 413 alloys.[10]

According to Anyalebechi,[5] the main drawback of

A.M. SAMUEL, Research Associate, and F.H. SAMUEL, Alcan-NSERC Industrial Research Chair Professor, are with the Department of Applied Sciences, University of Quebec at Chicoutimi, Chicoutimi, PQ, Canada G7H 2B1.

Manuscript submitted August 5, 1992.

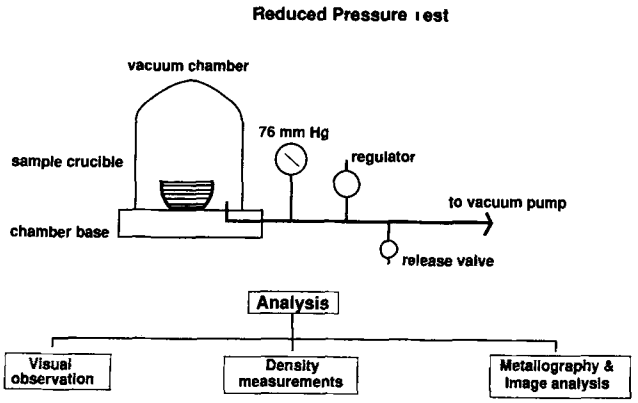

Fig. 1—Schematic representation of RPT apparatus and analysis.

this test is that it is insensitive to the very low hydrogen contents obtained/required in ingots prepared from properly filtered and degassed melts for fabrication purposes. Also, the results are influenced by the inclusions present in the melt.[11] Brondyke and Hess[11] have shown that removal of such inclusions affects bubble formation without changing the absolute hydrogen content, which can lead to misinterpretation of the results if the observed densities of the reduced pressure samples are related to the gas contents of their respective melts. Inclusions are known to act as nucleating agents that facilitate bubble formation during solidification of the sample under reduced pressure.

In the present work, the RPT was tested as a means of determining the hydrogen content in Al-Si-SiC(p) composite melts as part of an on-going study being carried out in our laboratories on such composites. With respect to ordinary Al alloy melts, the melting procedures followed for Al-Si-SiC(p) (Duralcan) composite melts differ in that no degassing or fluxing is allowed in the case of these melts[12] since these processes tend to remove the SiC particles, defeating the very purpose of the reinforcement. Also, while it is well known that the Telegas or Alscan and vacuum subfusion/fusion methods represent the most accurate means of hydrogen determination, the problems associated with probe blocking (due to the presence of the SiC particles) in the case of the former and the tedious analytical procedures involved in the latter necessitate the need for a more rapid, practical yet reliable method of doing so. This article reports on the qualitative and quantitative aspects of the results we have obtained from our study of the RPT on Al-7 wt pct Si-10 vol pct SiC composite. The qualitative results obtained show that in the case of composites also, the presence of oxide inclusions affects bubble formation similar to that reported by Brondyke and Hess.[11] However, the results can be reasonably interpreted, provided the density of the RP samples is related to the total porosity of these samples and not to their hydrogen contents.

II. EXPERIMENTAL PROCEDURE

A. *Materials and Melt Preparation*

The chemical composition of the F3A.10S designated composite alloy used in the present work is given in Table I and corresponds to the unreinforced A356 base alloy with a 10 (±2 vol pct) SiC content.

The material, supplied by Duralcan Canada (Québec) was received in the form of 12-kg ingots which were cut into small pieces (about 3-in. thick, long, and wide) and then melted in 7-kg capacity silicon carbide crucibles, using an electrical resistance heating furnace. The melt was continuously stirred mechanically, using a special impeller designed in our laboratory, to avoid SiC particle sedimentation. In each case, the melt temperature was maintained at 735 ± 5 °C before sampling.

The hydrogen content of the melts was varied by preparing melts using cold charges (containing more dirts and gases) as opposed to preheated charges and by introducing moisture (through spraying water) into the atmosphere above the melt. It must be remembered that being composite melts, no degassing or fluxing procedures could be employed as is done in the case of ordinary Al alloys as a means of reducing (*viz.*, varying) the hydrogen content.[12] Reduced pressure samples were also taken from the same melt at different stirring intervals. In some instances, oxide/inclusion content was deliberately enhanced by vigorous stirring of the melt.

B. *RPT Test Procedure*

The components of the RPT apparatus include a sample crucible, a vacuum chamber and base, a vacuum gage, a vacuum regulator, and a vacuum pump.[6] In the present study, a Gas-Tech II RPT unit manufactured by Stahl was used for carrying out the tests.[13] The uniquely designed vacuum chamber of the Gas-Tech II features a precision machined O-ring seat to assure a positive vacuum seal between the O-ring and the vacuum chamber base plate. A twin diaphragm vacuum pump can quickly obtain up to 28.5 in. of Hg vacuum. A precalibrated gage assures that the reduced pressure is maintained at a particular value corresponding to a specified gage reading (*e.g.*, 50 torr at 28-in. Hg vacuum). The heavy duty coupon crucibles (or sampling cups) supplied with the unit were preheated in a furnace at 400 °C prior to sampling. A sample of molten alloy was removed from the melt to the cup, the cup placed in the vacuum chamber, and its contents allowed to solidify under reduced pressure. The pressure (except in some cases) was maintained at 76-mm Hg for all the reduced pressure (RP) samples prepared from different melts. Atmospherically solidified cup samples were also prepared from the same melts for comparison and standardization purposes. Two to three samplings were done for each condition. All samplings were carried out within two consecutive days under the same atmospheric conditions.

For determining the hydrogen content of the melts, samples were simultaneously cast in a Ransley mold (specially designed to prepare castings that are porosity free and which retain the hydrogen content of the melt in the solidified sample[14]), from which "Ransley" samples were machined and sent for hydrogen analysis using the LECO* or vacuum fusion method.[15] This is one of the standard methods for obtaining accurate analysis of the hydrogen content in a melt. The LECO analysis was

*LECO is a trademark of LECO Corporation, St. Joseph, MO.

Table I. Chemical Composition of Al-Si-SiC(p) Composite Alloy

Composite Alloy	Chemical Composition of Al-Si Matrix Alloy (Wt Pct)							SiC (Vol Pct)
	Si	Fe	Cu	Mn	Mg	Ti	Sr	
F3A.10S	7.45	0.13	0.019	0.003	0.40	0.10	0.014	11.30

carried out at Alcan International's Arvida R&D Centre in Jonquière, Québec.

C. *Sample Analysis*

The densities of the RP and atmospherically solidified samples were determined, using the Archimedes principle, from the weights of the samples taken in air and in water. Precautions were taken to ensure that all weights were determined under identical conditions. The samples were then cut in half along the transverse direction and the cut surfaces examined for porosity after the proper procedures for polishing such composites were carried out. Photographs of the cut surfaces were also taken for visual assessment. Image analysis (LECO 2001 image analyzer, in conjunction with an Olympus PMG3 optical microscope) was employed to measure the porosity content and various aspects of the porosity, *viz.*, shrinkage, gas, and microporosity, as well as pore size and distribution. Details of image analysis measurements are given in Section III, with respect to Figures 4 and 9, in the appropriate context.

The different types of porosity observed in the samples, namely, shrinkage, gas, and microporosity, were defined and distinguished as follows:[16]

Shrinkage pores: large pores encompassing many dendrites and having a shape typically that shown by Figure 2(a), but with much larger sizes; large shrinkage pores usually appear in the shrinkage pipe or upper region (riser part) of a casting (*cf.* case for composite samples, Figure 4).

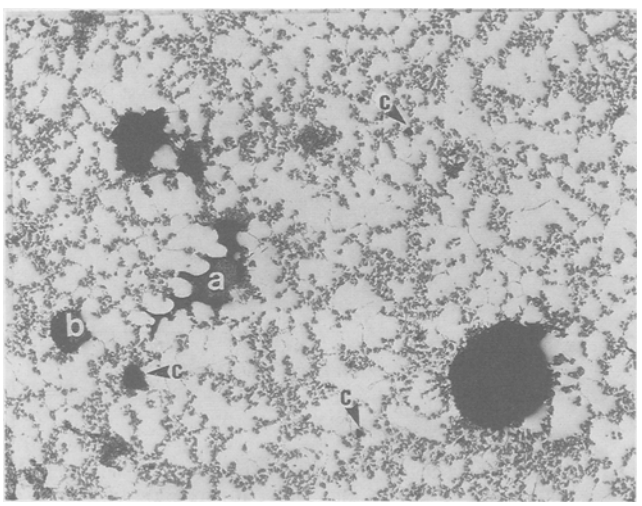

Fig. 2—Micrograph taken from an F3A.10S reduced pressure composite sample, showing typical examples of the different types of pores observed (magnification 200 times): (*a*) shrinkage pore, (*b*) gas pore, and (*c*) microporosity.

Gas pores: due solely to gas and represented by the round pore shown by Figure 2(b).

Microporosity: representing the vast majority of pores encountered due to a combination of gas and shrinkage; these pores occur typically in the interdendritic regions and can vary in size from a few up to several hundred microns (Figure 2(c)).

It should be mentioned here that since almost all porosity is usually due to a combination of gas and shrinkage, distinction between the different types was mainly made on the basis of size as well as the shape of the pores.

III. RESULTS AND DISCUSSION

A. *Quantitative Analysis of the RP Test*

The quantification of the RP test as initially presented by Rosenthal and Lipson[7] involves the concept of utilizing reduced pressure solidification and density measurements to quantitatively measure the gas (hydrogen) content of an aluminum alloy melt. From measurements of the densities of RP samples, the porosity content in these samples is estimated and then related to their hydrogen content *assuming all of the porosity is due to hydrogen*. The hydrogen content [H] (in mL/100 g Al) is then determined from the relationship

$$[H] = K\,(1/D_{rp} - 1/D_{th}) \qquad [1]$$

where D_{rp} is the density of the reduced pressure sample, D_{th} is the theoretical density of the alloy, and the RP measurements are standardized to STP conditions through the gas law constant, K,

$$K = P_2/760 \times 273/T_2 \times 100 \qquad [2]$$

where P_2 and T_2 are the reduced pressure (mm Hg) and the alloy solidus temperature (deg K), respectively.

Parallel to Eq. [1], other workers[4,17] use the "porosity index" (or, more correctly, the "indice de gazage") defined as

$$i = 1000\,(1/D_{rp} - 1/D_{th}) \qquad [3]$$

to judge the gas content of an alloy melt, with values of 0 to 10, >20, and >50, representing low, medium, and high gas levels, respectively.

However, as Sulinski and Lipson[8] and, recently, Gruzleski and co-workers[9,10] have pointed out, the simple formula of Eq. [1] automatically assumes that all the hydrogen present in the liquid melt forms pores in the solid, that no hydrogen is lost during evacuation, and that the gas forms at the solidus temperature of the alloy at the specified reduced pressure. As such, therefore, a correct estimation of the hydrogen content cannot be made on the basis of Eq. [1]. In fact, it is precisely these

factors, *viz.*, vacuum measurement, pressure reduction, and solidification mechanism that affect RPT results[6] and on which its success as a measuring tool is hinged.

Based on studies involving actual measurements of the melt hydrogen using the Telegas method, Gruzleski's group demonstrated the possibility of obtaining hydrogen values close to the real (Telegas) values when a correction factor originally proposed by Rosenthal and Lipson[7] was applied to the hydrogen values calculated from the RP samples of A356 alloy. This correction factor, defined as the ratio of the hydrogen contents of atmospherically solidified and RP samples (from the same melt), is calculated from Eq. [1].

In the present study, the actual hydrogen content was analyzed by means of the vacuum fusion (LECO) method. The solidus temperature for the F3A.10S alloy was determined to be 608 °C from studies carried out in our laboratory.[18] The theoretical density as reported in the literature is 2.7011 g/cm^3.[12] Using this data, various calculations were executed to determine the correlation between hydrogen content, density, and porosity. The results have been reported elsewhere[19] in detail and are summarized here in Figure 3. As can be seen, there is a definite linear relationship between density and hydrogen content for the reduced pressure samples, the values, although scattered, still lying within a narrow band (Figure 3(a)). In comparison, the decrease in density is less marked for the atmospherically solidified (or "air") samples (Figure 3(b)). This is expected, as the reduced pressure magnifies the hydrogen porosity, whereas there is no such effect in the case of the air samples. Also, in Figure 3(a), the decrease is more marked at higher hydrogen levels, indicating that gas is evolved and lost from the sample during reduced pressure solidification. Figure 3(c) shows the porosity index *vs* hydrogen content plots for RP (open symbols) and air (bold symbols) samples of F3A.10S. The RP samples exhibit a relation very similar to that obtained by Laslaz and Laty for A356 alloy.[4] The air samples exhibit very low values of porosity index (<10) over the entire hydrogen range, as expected.

Figure 4(a) shows the density *vs* hydrogen plots for calculated, corrected, and measured (LECO) values of hydrogen content for F3A.10S RP samples, following the procedure outlined by La Orchan *et al.*[10] No agreement between the corrected and measured hydrogen values is observed, suggesting that the application of a correction factor, as defined by Rosenthal and Lipson, is incorrect and that other specifics of the composite alloy must also be taken into account. Referring to the A356 and 413 alloys studied by La Orchan *et al.*[10] and the fact that while the Rosenthal-Lipson correction factor applied in the case of A356 and did not for 413 because of the differences in the solidification behaviors of the two alloys, the same reasoning may also be applied in the present case to the observed lack of correlation.

From considerations of the density values, actual melt hydrogen levels (LECO), and calculated hydrogen values (derived from the Rosenthal-Lipson procedure), a simple fitting of the data obtains individual correction factors of 5.96 and 3.15 (average values) for melt hydrogen levels of 0.2 and 0.3 mL/100 g, respectively (Table II).

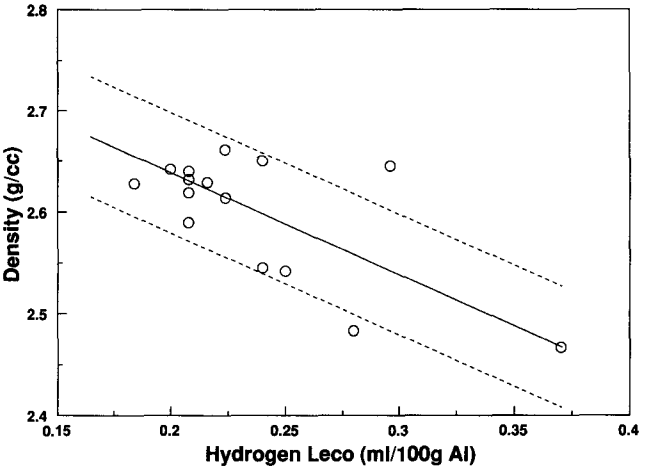

(*a*)

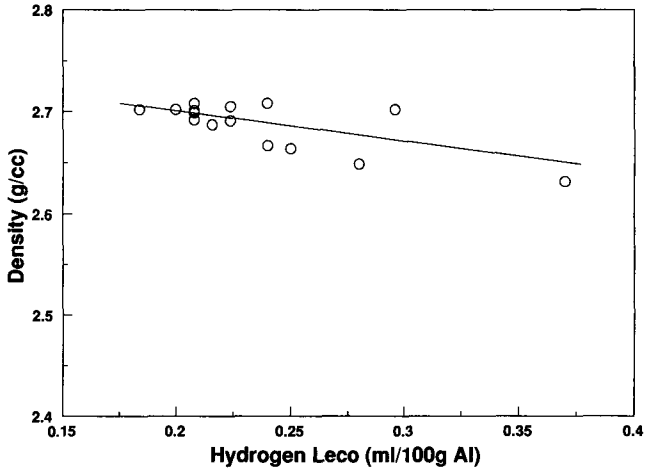

(*b*)

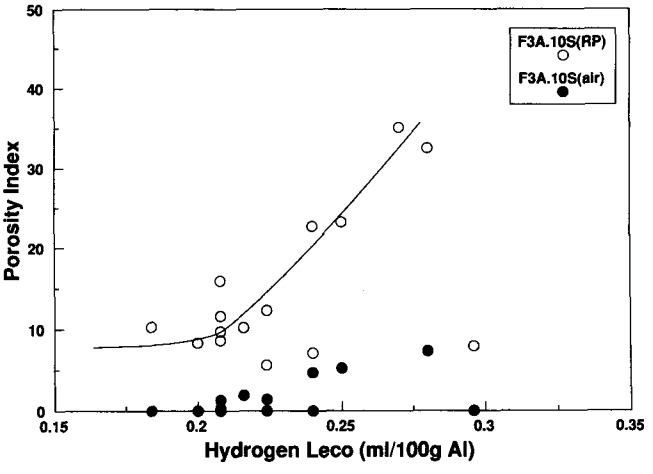

(*c*)

Fig. 3—Plots of (*a*) and (*b*) density and (*c*) porosity index *vs* hydrogen content for (*a*) reduced pressure (76-mm Hg) solidified, (*b*) atmospherically solidified, and (*c*) reduced pressure and atmospherically solidified F3A.10S composite samples.

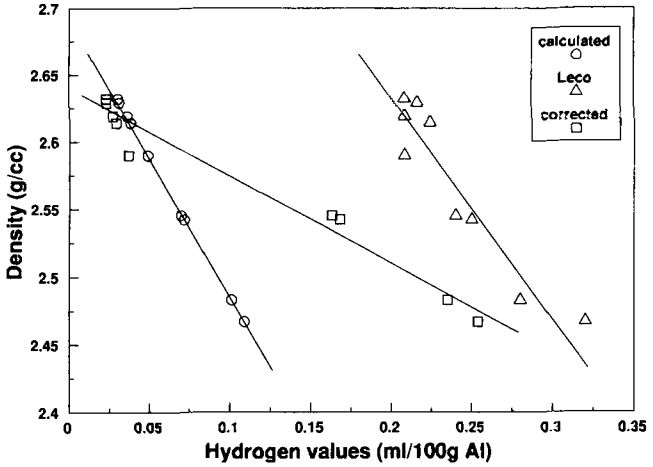

(*a*)

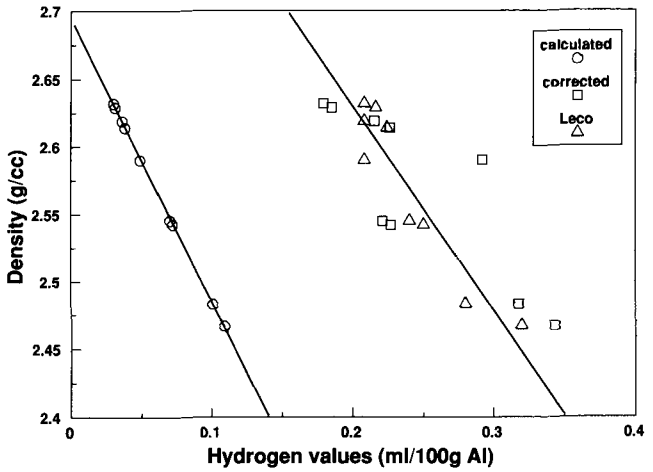

(*b*)

Fig. 4—Density *vs* hydrogen plots for calculated, corrected, and measured (LECO) values of hydrogen contents for F3A.10S reduced pressure solidified samples, showing corrected values obtained using (*a*) the Rosenthal-Lipson correction factor and (*b*) correction factors as proposed in the present work.

The results of Table II, plotted in Figure 4(b) for comparison with Figure 4(a), indicate that one cannot assume an average correction factor throughout the range of hydrogen levels exhibited by different melts. Apparently, even for the range 0.15 to 0.30 mL/100 g Al, the correction factor appears to be a function of the hydrogen level unlike that reported for the case of A356 alloy by La Orchan *et al.*, according to whom the correction factor is not a strong function of the hydrogen level within this range.

An attempt to characterize an appropriate correction factor that would provide an understanding of the physical phenomena involved during the solidification of the alloy would require testing a considerably large number of samples, prepared from melts covering a broad range of hydrogen levels, to arrive at any reasonable formulation or value of said correction factor. Since not enough statistical data was obtained in the present work on both counts, no attempt is made to propose any correction factor at this stage. All that can be said is that the correction factor definitely appears to be a function of the hydrogen level of the melt.

Figure 4(a) also shows that the densities of the RP samples cannot be related to the hydrogen content/porosity of their melts alone but must be, more correctly, related to the total porosity of the sample, which includes both shrinkage and microporosity in addition to gas porosity. The shrinkage porosity was observed to be mostly concentrated in a denuded zone (free of SiC particles), usually 1 to 3-mm thick at the top of the cup sample as well as down the length of the sample in the central region of the cut surface, what would normally be the shrinkage cavity area in such a casting. Measurements of porosity (using image analysis) were therefore made separately for areas *A* and *B* shown in Figure 5. For area *B*, 200 fields were analyzed, covering an average area of 42 × 22 mm, while the denuded zone, area *A*, representing the major part of the shrinkage porosity, required about 50 fields (the term "field" representing the field of view of the optical microscope used in conjunction with the image analyzer to measure the porosity and covering an area of 1.61242×10^5 sq microns at a magnification of 200 times). The number of fields examined was chosen such that the specimen area was traversed in a regular, systematic fashion and covered entirely by the respective number of fields, following the procedures adopted by Alcan International's Arvida R&D Centre for the measurements of ceramic and porosity volume fractions in composites by image analysis.[20] The total porosity was then determined from the average values obtained from the image analysis results and the areas of the respective parts.

Figure 6 shows plots of (a) gas porosity *vs* hydrogen content and (b) total porosity *vs* density for the RP samples of F3A.10S composite. It is seen that a much more reasonable correlation is obtained when the total porosity is taken into consideration (with the values lying within the band defined by the dashed lines). Thus, the RPT is a better indicator of the porosity content of the sample rather than of the true hydrogen content of its melt, and it is this porosity content that should correctly relate to the measured density (as is observed in Figure 6(b)). Hydrogen porosity, related to the hydrogen content, represents only part of the porosity picture.

In this context, it is interesting to note that other workers (*e.g.*, Laslaz and Laty of the Pechiney group) consider RPT density measurements as "representative of the alloy porosity," whereas hydrogen contents are measured using the Telegas apparatus and not calculated from the former.[4] Also, at the time when density measurements appeared an attractive means of assigning quantitative ratings to RP samples and the quantification procedures that followed,[7,8,21] Brondyke and Hess[11] were probably the only ones to point out the lack of correlation between densities of aluminum alloy reduced pressure samples and the hydrogen contents of their melts, ascribing the discrepancy to the presence of inclusions and cleanliness of the melt in general.

Very recently, DeWeese *et al.*[22] have also indicated the utility of the RPT as a means of evaluating "hydrogen gas *presence*" and its subsequent effect on the porosity of the casting. According to them, the relationship

Table II. Hydrogen Values Obtained from F3A.10S Reduced Pressure Samples and Their Melts

Sample Density (g/cc)	Calculated H_2 Value (mL/100 g Al)	Actual Melt H_2 (mL/100 g Al)		Correction Factor		Corrected H_2 Value (mL/100g Al)
2.629	0.031	0.216	average: 0.2	6.97	average: 5.96	0.185
2.614	0.038	0.224		5.89		0.226
2.590	0.049	0.208		4.24		0.292
2.619	0.036	0.208		5.78		0.215
2.632	0.030	0.208		6.93		0.179
2.467	0.109	0.32	average: 0.3	2.94	average: 3.15	0.343
2.483	0.101	0.28		2.77		0.318
2.542	0.072	0.25		3.47		0.227
2.545	0.070	0.24		3.43		0.221

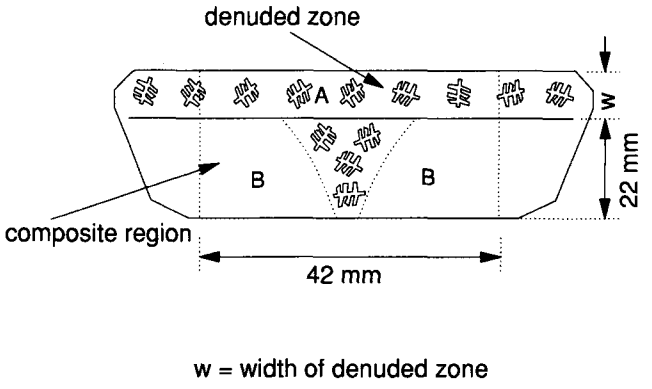

Fig. 5—Schematic diagram depicting the cut cross section of a typical reduced pressure (or air) sample. Shrinkage porosity (denuded zone) and other porosity (composite region) were measured over areas *A* and *B* as shown.

between porosity and density is evidenced from the relation

$$P = [1 - D_{bulk}/D_{nom}] \times 100 \quad [4]$$

for determining the percentage of volume porosity, with D_{bulk} and D_{nom} representing the bulk and theoretical densities, respectively. The difference between the two can give a close approximation of the amount of internal hydrogen porosity present in the melt. Of importance to note is that D_{nom} would vary according to the composition of the alloy.

Equation [4] was applied in the present case and P values calculated for the sample density (D_{bulk}) values mentioned in Table II. Absolute values of $P - D_{bulk}$ were then plotted *vs* the actual melt hydrogen levels, as shown in Figure 7. The straight line representing the linear regression fit of the plotted points indicates that $P - D_{bulk}$ can indeed be related to the hydrogen porosity (*i.e.*, hydrogen content), as proposed by the authors. Physically speaking, this makes more sense rather than the Rosenthal-Lipson approach of relating density to the hydrogen content.

B. *Qualitative Analysis of the RP Test*

Figures 8(a) and (b) show the cut surfaces of F3A.10S samples obtained from the same melt under (a) atmospheric solidification and (b) 76-mm Hg reduced pressure. The reduced pressure mainly serves to magnify the

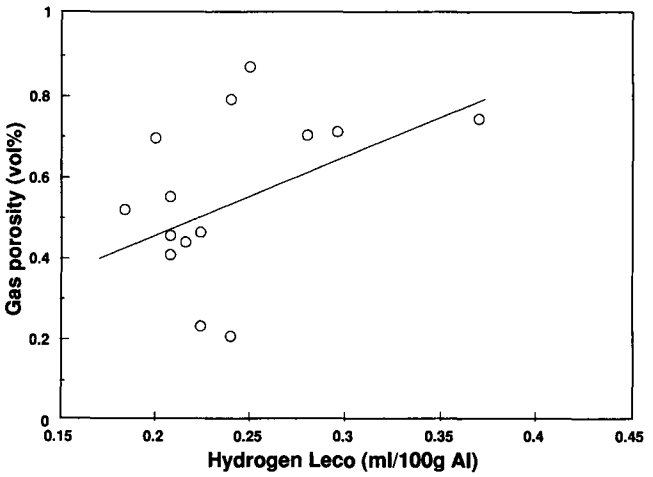

(*a*)

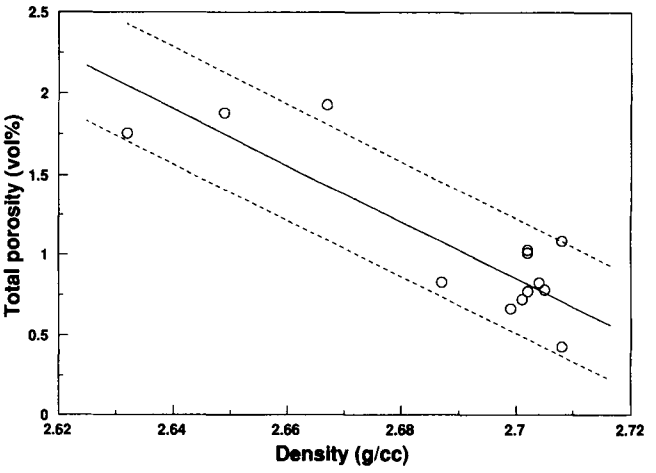

(*b*)

Fig. 6—Plots of (*a*) gas porosity *vs* hydrogen content and (*b*) total porosity *vs* density for F3A.10S reduced pressure solidified samples.

size of the porosity (mostly gas) but not the distribution or the content. This is brought out very clearly by the porosity count *vs* area distribution graphs shown in Figure 9 for air and RP samples obtained from the same melt. Based on the limits of the image analyzer system (neither automated nor programmed to prevent cutting off of pores during analysis), two ranges of porosity were measured: (a) pores whose area ranged from 0 to

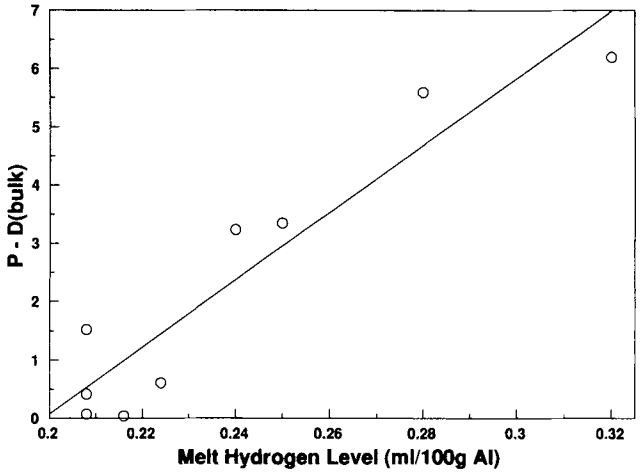

Fig. 7—Plot of P-D_{bulk} *vs* melt hydrogen level for reduced pressure samples of F3A.10S, showing their linear relationship (see Section III-A, Equation [4] for details).

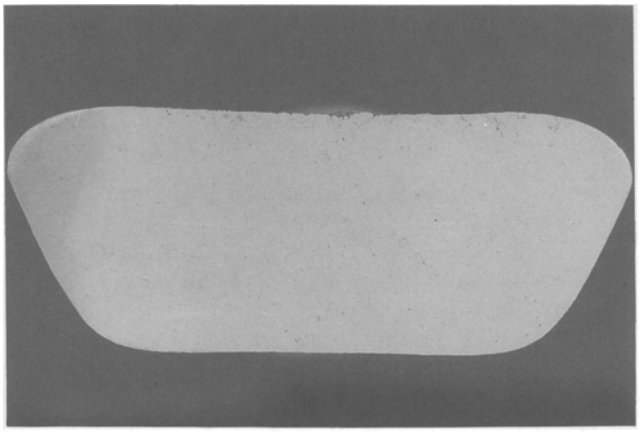

(*a*)

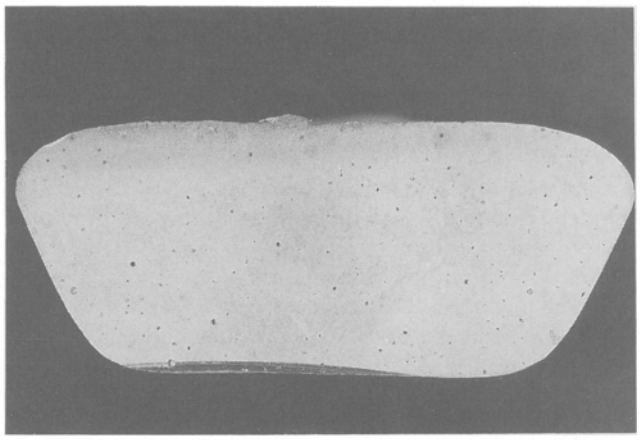

(*b*)

Fig. 8—Cut cross sections of F3A.10S samples obtained from the same melt under (*a*) atmospheric and (*b*) 76-mm Hg reduced pressure solidification.

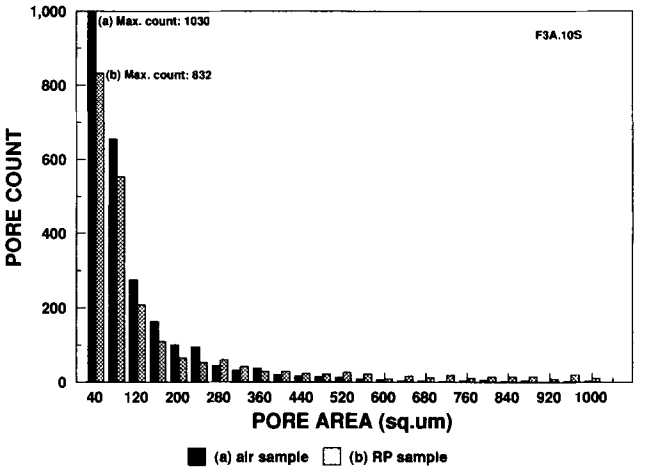

(*a*)

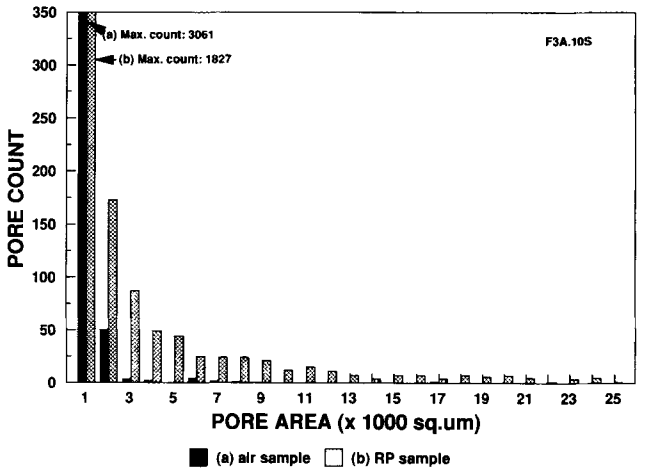

(*b*)

Fig. 9—Pore size and distribution graphs for F3A.10S composite samples obtained under (a) atmospheric solidification (black bars) and (*b*) 76-mm Hg reduced pressure (cross-hatched bars) in the ranges (*a*) 0 to 1000 sq micron and (*b*) 0 to 25,000 sq micron.

1000 sq microns and (b) pores whose area ranged from 0 to 25,000 sq microns. The former range was chosen to cover and elaborate upon the microporosity aspects and the latter to reflect the amount of shrinkage porosity in a particular sample. With respect to the porosity distribution graphs shown in Figure 9 and subsequent figures, it should be pointed out that while the Y-axis represents pore count, it is essentially a form of pore density that is being measured, since all the measurements were done over a fixed area (42 × 22 mm) and a fixed number of fields of observation chosen (200 fields) to cover this area in a regular, systematic fashion.[20]

Figures 10(a) and (b) compare the cut surfaces of F3A.10S and A356 matrix alloy reduced pressure samples. The difference in the shape and nature of the porosity is evidenced for the two types of materials. In the matrix alloy, the pores nucleate in the interdendritic regions and, often, adjacent individual interdendritic pores merge, one into the other, over several dendrite lengths, giving rise to what appears to be shrinkage-type porosity but which is actually due to both gas and shrinkage

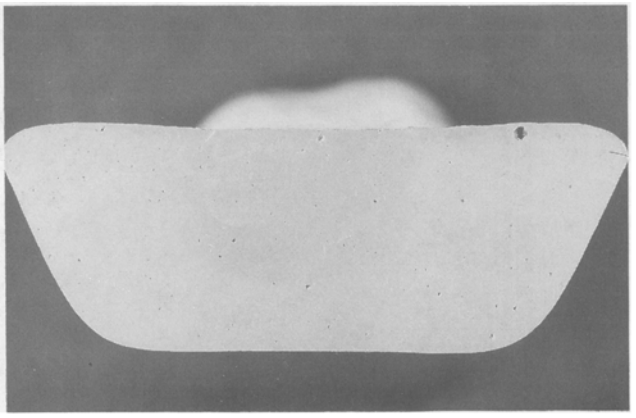

(*a*)

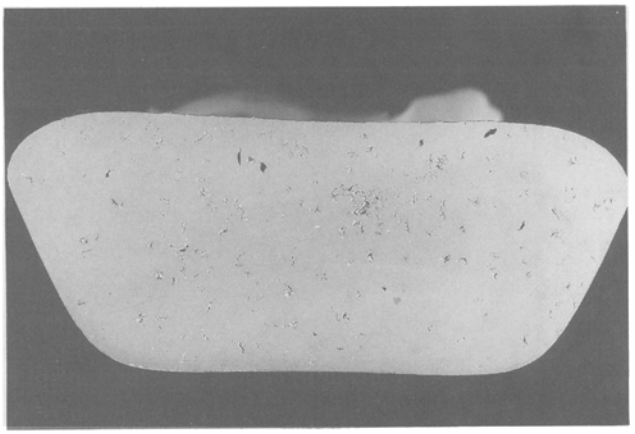

(*b*)

Fig. 10—Cut cross sections of (*a*) F3A.10S and (*b*) A356 reduced pressure (76-mm Hg) samples.

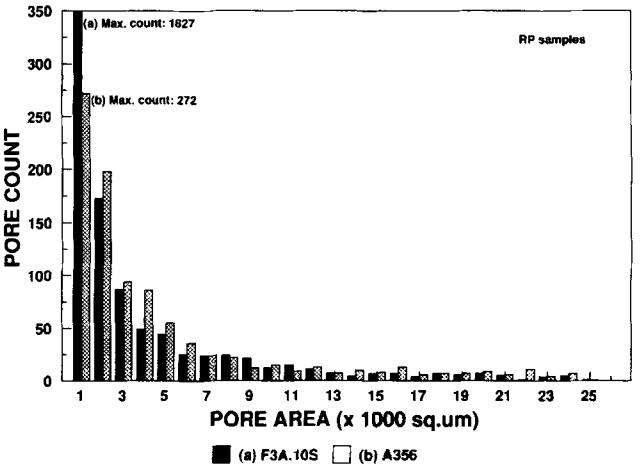

Fig. 11—Pore size and distribution chart for (*a*) F3A.10S and (*b*) A356 reduced pressure (76-mm Hg) samples.

(Figure 12(b)). This leads to the larger, extended pores visible in Figure 10(b). In the composite specimen, on the other hand, the porosity appears as pinholes distributed over the entire surface in a relatively even manner (Figure 10(a)).

Figure 11 displays the porosity distributions observed for the RP samples taken from F3A.10S and A356 alloy melts. Comparison between the two distributions clearly indicates the much larger pores that exist in the matrix alloy sample. Of interest to note is that the reduced pressure does not affect the shrinkage (larger-sized) pores. The gas pores falling within the (0 to 2000) sq micron range, though, are affected by the reduction in pressure.

In a parametric study of the evolution of microporosity in Al-Si foundry alloys, Tynelius[23] performed statistical analyses to describe the size and amount of porosity as a function of alloying and process variables in A356.2 alloy, where the area percent porosity, maximum pore area, and areal pore density were measured by image analysis. The pore size distributions could be divided into three types: in type I, the pore size distribution was skewed toward small pore sizes; in type II, both relatively small and large pores were present in the sample; and in type III, the pore size distribution was skewed toward large pore sizes (for pore areas ranging from 0 to 5×10^5 mm^2) (Tynelius,[23] Figure 53, p. 123). Taking into account the hydrogen content and local solidification time, among other parameters, and the number of pores obtained in each type, the three types of distribution were then described as follows:

type I—porosity resulting mainly from nucleation of pores;
type II—porosity formed by nucleation and growth of pores; and
type III—porosity increasing mainly due to growth and coarsening of pores.

It was shown that the hydrogen content was the most important factor for the size and amount of microporosity in A356.2 alloy castings, with the results indicating that subsequent growth is diffusion controlled and that there is a critical radius for growth of a pore nucleus, which is a function of fraction solid, metal pressure, hydrogen content, and time, unique to each alloying condition.

The pore size distributions presented here (Figures 9 and 11 as well as Figures 14 and 15 later) are all seen to be type I distributions, *viz.*, the porosity results mainly from the nucleation of pores. This is to be expected because of the SiC particles present in the matrix alloy, where there is a tendency for pores to nucleate at the sites of these particles (as shown in Figure 12(d)). This leads to larger amounts of microporosity in the composite samples compared to the matrix A356 alloy sample. On the other hand, we have also observed the tendency of the SiC particles to restrict pore growth. A combination of these two factors accounts for the typical skewed distributions observed in the present studies. Of interest to note is the range of pore sizes (0 to 25,000 sq microns) in the case of composites and that reported by Tynelius for A356.2 (0 to 500,000 sq mm).[23] The medium to high hydrogen contents of the composite melts reported here and the shorter solidification times involved (7 to 8 minutes) would also support a type I distribution.

Figures 12(a) and 12(b) show the microstructures corresponding to Figures 10(a) and 10(b), respectively. In Figure 12(a), the pores are seen to be rounder and

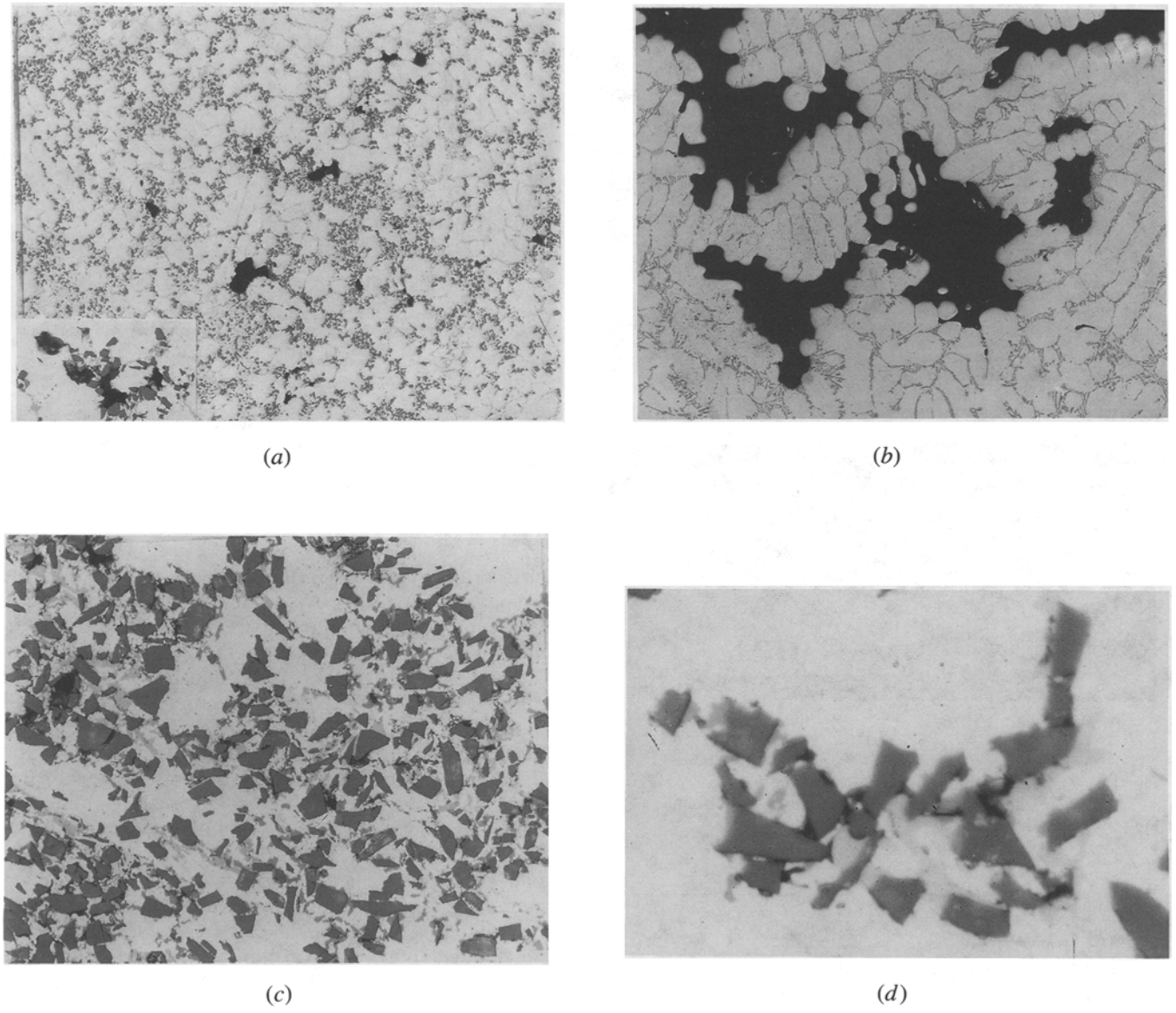

Fig. 12—Microstructures corresponding to the (*a*) F3A.10S and (*b*) A356 reduced pressure solidified samples shown in Fig. 10 (magnification 50 times). The inset in (*a*) shows how the SiC particles restrict the growth of the pores (magnification 200 times). This tendency is further exemplified in the higher magnification (magnification 500 times) micrograph shown in (*c*), while the nucleation of fine pores at SiC particle sites is clearly seen in (*d*), taken at magnification 2000 times.

smaller and never spread across adjoining lengths of interdendritic regions. The inset, taken at a higher magnification (200 times), shows how the SiC reinforcement particles have a tendency to restrict the growth of the pores, as they are always found to appear surrounding the pores. This was found to be the case for all composite specimens and for all types of pores, including those due to shrinkage and oxide inclusions, as shown clearly by the higher magnification (500 times) micrograph of Figure 12(c). A still higher magnification micrograph (2000 times) shows how the porosity appears associated with the SiC particles in the form of very fine microporosity.[24] It is this tendency that results in SiC(p) reinforced Al alloy composites displaying large amounts of microporosity when compared to composites reinforced with other types of particles, *e.g.*, Al_2O_3.

Figures 13(a) and (b) correspond to the cut surfaces of F3A.10S composite RP samples taken from melts containing (a) oxides and dirts and (b) a high hydrogen content, respectively. At first glance, the two surfaces appear to be similar, but it is possible to discern some distinguishing features. The pores in the oxide containing melt are larger than those observed in the high hydrogen melt and the porosity content much greater, in spite of the latter having a higher hydrogen content (0.3 *vs* 0.2 mL/100 g). The corresponding porosity distributions shown in Figure 14 support these observations. The high hydrogen melt displayed a tendency for greater microporosity, as was observed during the measurements and evidenced by the (0 to 1000) sq micron section of the porosity distribution graph shown in Figure 14. The porosity distribution graph of the air samples of these melts (Figure 15) also revealed that the high

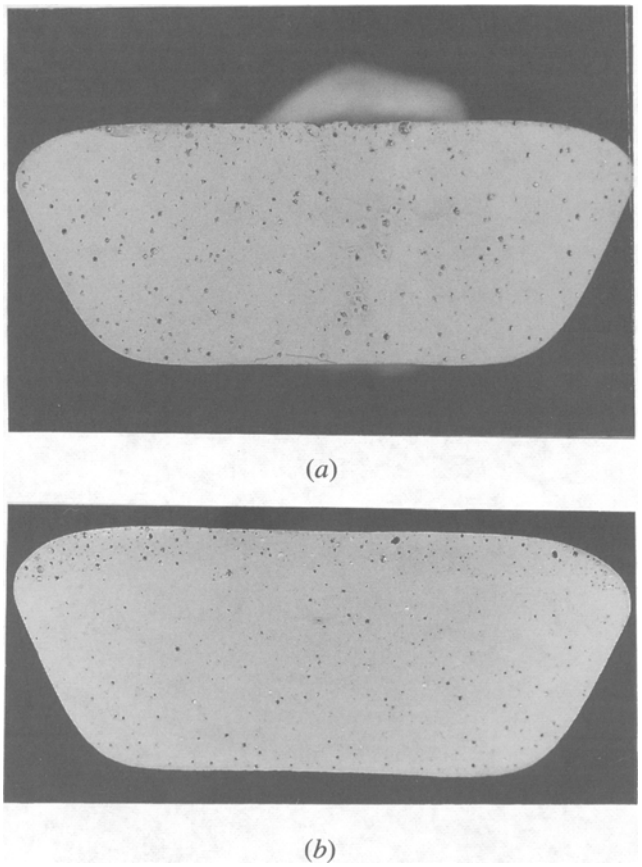

Fig. 13—Cut cross sections of reduced pressure F3A.10S composite samples taken from melts containing (*a*) oxides and dirts and (*b*) a high hydrogen content.

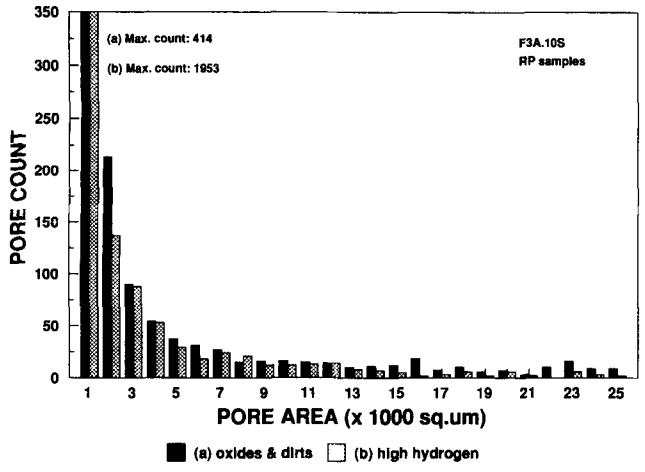

Fig. 14—Pore size and distribution graphs for the reduced pressure samples shown in Fig. 13: (*a*) black bars, corresponding to Fig. 13(a), and (*b*) cross-hatched bars, corresponding to Fig. 13(b).

hydrogen melt displayed the greater microporosity, particularly in the (0 to 120) sq micron range. High hydrogen melts are known to display a large amount of microporosity.[1,23]

Another point of interest to note in the high hydrogen sample is that with the application of the reduced pressure, the hydrogen gas pores are drawn up to the top

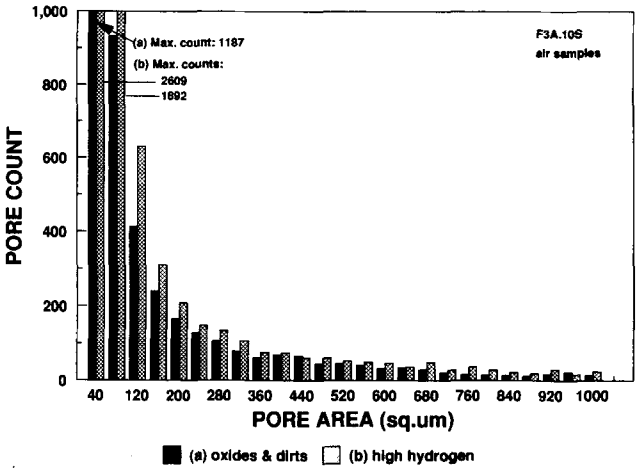

Fig. 15—Pore size and distribution graph for the air samples taken from the same melts corresponding to Fig. 13: (*a*) black bars, oxide containing melt, and (*b*) cross-hatched bars, melt with the high hydrogen content.

surface and segregate in the denuded zone area of the sample (Figure 13(b)). No such effect is observed in the oxide containing sample (Figure 13(a)). The oxide inclusions have a tendency to trap the hydrogen at the sites where they occur. Although different Al oxides may be present, many of them have densities close to that of aluminum. Hence, even with the application of the reduced pressure, these would remain embedded within the matrix. Figure 16 displays a magnified view of this effect: the reduced pressure samples of F3A.10S clean and oxide-containing melts obtained at a much lower pressure of 25-mm Hg show clearly (a) the effect of the reduced pressure on the gas porosity; (b) how the gas containing pores are all drawn up to the top surface of the solidifying sample in the case of the clean melt sample (Figure 16(a)); and (c) how many of the same gas pores are embedded within the matrix when a number of oxide inclusions are present in the melt (Figure 16(b)) to trap them.

It has been reported that nonmetallic inclusions aid in the nucleation of hydrogen absorption and coalescence within the material.[25] Thus, even for a melt with a relatively low hydrogen content, the presence of these oxides (and other inclusions) can increase the porosity tremendously. This is clearly brought out when one compares the samples obtained from melts containing similar hydrogen levels (0.2 mL/100 g), but one dirty and the other clean (Figures 13(a) and 10(a), respectively), with that shown in Figure 13(b) for the high hydrogen melt sample. The oxide containing sample exhibits a porosity comparable to or even greater than the high hydrogen sample (*cf.* Figures 14(a) and (b)).

IV. CONCLUSIONS

Summarizing the situation, after analysis of the measurable parameters (density, hydrogen content, and porosity) and using the various quantification procedures provided in the literature, the following are found.

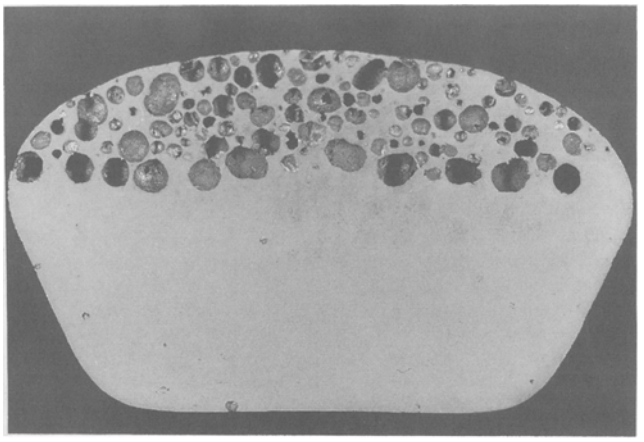

(*a*)

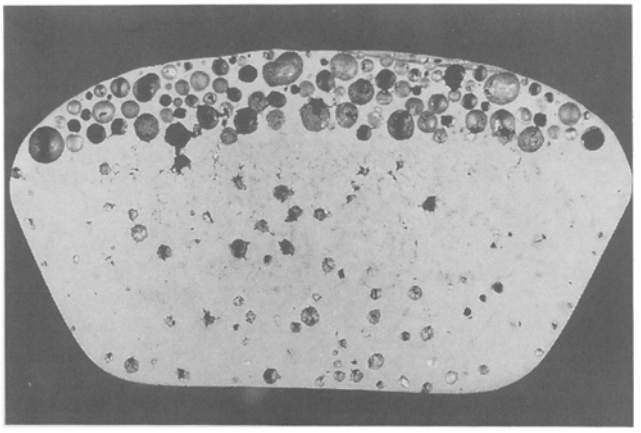

(*b*)

Fig. 16—Cut cross sections of F3A.10S composite samples obtained at 25-mm Hg reduced pressure, showing (*a*) how the hydrogen gas pores segregate to the top surface of the sample in the absence of oxides in the melt and (*b*) how the oxide inclusions present in the melt trap these hydrogen gas pores at the sites where they occur within the matrix.

1. The reduced pressure test does not indicate the true hydrogen content of the melt in the case of the Al-7 wt pct Si-10 vol pct SiC(p) composite studied. Instead, it is a better and more appropriate indicator of the porosity content in the sample, reflecting the effects of both shrinkage and gas porosity, as well as the cleanliness of the melt.
2. As it is the porosity that ultimately affects the performance of a casting in terms of its properties and soundness, the importance of this test should be reoriented, with the density measurements being related to the *porosity* rather than the *hydrogen* content.
3. Qualitative aspects of the RPT also affirm that it is a reasonably good indicator of melt quality in terms of the oxide inclusions and hydrogen content that affect the porosity obtained in the solidified composite sample. These observations are substantiated throughout in the present work by the pore size and distribution data obtained from image analysis.
4. It has been seen in this study how the porosity shape and size are affected by the presence of the SiC reinforcement particles through the tendency these particles display to block or restrict the growth of the pores. As a result, a more uniform distribution of porosity is obtained compared to the unreinforced matrix alloy (A356) where the porosity is seen to occur in the interdendritic regions that can easily spread across several dendrites when adjacent pores merge into each other, leading to very large pore sizes. In this sense, the composite material is seen to have a beneficial effect on the growth of porosity.
5. There is a tendency for pores to nucleate at the sites of the SiC particles. The associated microporosity observed in such types of SiC(p) reinforced Al alloy composites, together with the tendency of the SiC particles to restrict the growth of the pores, results in the skewed pore size distribution curves typically obtained for the composite samples studied, conforming to the type I distributions obtained for A356.2 alloy[23] where the porosity results mainly from nucleation of pores.

Thus, despite the difficulties encountered in the quantification of the RP test, it can nonetheless be fruitfully employed to indicate the expected quality of a casting in terms of the porosity content and other features described previously.

ACKNOWLEDGMENTS

The authors would like to thank Dr. H. Liu for his help during the course of this work and Dr. J. Boutin of ARDC, Alcan International Ltd., Jonquière, for the LECO hydrogen analyses. The financial support received from the Natural Sciences and Engineering Research Council of Canada, the Fondation Sagamie de l'Université du Québec à Chicoutimi, and the Societé d'électrolyse et de chimie Alcan (SECAL) is gratefully acknowledged.

REFERENCES

1. D.E.J. Talbot: *Int. Metall. Rev.*, 1975, vol. 20, pp. 166-84.
2. D.V. Neff and P.V. Cooper: *AFS Trans.*, 1990, vol. 98, pp. 579-84.
3. H. Iwahori, K. Yonekura, Y. Yamamoto, and M. Nakamura: *AFS Trans.*, 1990, vol. 98, pp. 167-73.
4. G. Laslaz and P. Laty: *AFS Trans.*, 1991, vol. 99, pp. 83-90.
5. P.N. Anyalebechi: *Light Met.*, 1991, pp. 1025-46.
6. W. Rasmussen and C.E. Eckert: *Modern Casting*, 1992, March, pp. 29-31.
7. H. Rosenthal and S. Lipson: *AFS Trans.*, 1955, vol. 63, pp. 301-05.
8. H.V. Sulinski and S. Lipson: *AFS Trans.*, 1969, vol. 67, pp. 56-64.
9. M.H. Mulazimoglu, N. Handiak, and J.E. Gruzleski: *AFS Trans.*, 1989, vol. 97, pp. 225-32.
10. W. La Orchan, M.H. Mulazimoglu, and J.E. Gruzleski: *AFS Trans.*, 1991, vol. 99, pp. 653-59.
11. K.J. Brondyke and P.D. Hess: *Trans. TMS-AIME*, 1964, vol. 230, pp. 1542-46.
12. *Duralcan Composite Casting Guidelines*, Duralcan USA, San Diego, CA, 1990, VIII-1.
13. T.E. Acklin and N.J. Davidson: *Proc. 2nd Int. Conf. on Molten Aluminum Processing*, Orlando, FL, Nov. 6–7, 1989, American Foundrymen's Society, Des Plaines, IL, 1989, pp. 19.1-19.10.
14. C.E. Ransley and D.E.J. Talbot: *J. Inst. Met.*, 1955–1956, vol. 84, pp. 445-52.

15. C. Dupuis, Z. Wang, J.-P. Martin, and C. Allard: *Light Met.*, 1992, pp. 1055-68.
16. J.E. Gruzleski and B.M. Closset: *The Treatment of Liquid Aluminum-Silicon Alloys*, The American Foundrymen's Society, Inc., Des Plaines, IL, 1990, pp. 149-52.
17. S. Jacob and M. Richard: *Fonderie-Fondeur d'Aujourd' hui*, 1986, Oct. (58), pp. 10-21.
18. A. Labib, H. Liu, and F.H. Samuel: *AFS Trans.*, 1992, vol. 100, pp. 1033-41.
19. A.M. Samuel and F.H. Samuel: *Advances in Production and Fabrication of Light Metals*, M.M. Avedesian, L.J. Larouche, J. Masounave, eds., The Metallurgical Society of the Canadian Institute of Mining, Metallurgy and Petroleum, Montreal, 1992, pp. 701-15.
20. J. Boutin and C.E. Gallernault: Report No. AR-89/0028, Arvida R&D Centre, Alcan International Limited, Jonquière, Quebec, Canada, July 1989.
21. J.C. Church and K.L. Herrick: *AFS Trans.*, 1970, vol. 78, pp. 277-80.
22. S.K. DeWeese, R. Atkinson, and W. Rasmussen: *Modern Casting*, 1992, April, pp. 29-31.
23. K. Tynelius: Ph.D. Thesis, Drexel University, Drexel, Philadelphia, PA, Mar. 1992.
24. D.J. Lloyd and B. Chamberlain: *Cast Reinforced Metal Composites*, S.G. Fishman and A.K. Dhingra, eds., ASM INTERNATIONAL, Chicago, IL, 1988, pp. 263-69.
25. J. Jorstad: *Die Cast. Eng.*, 1986, Nov.–Dec., p. 30.